



**HAL**  
open science

## EEG signals analysis for epileptic seizures detection using polynomial transforms, linear discriminant analysis and support vector machines

Laurent Chanel Djoufack Nkengfack, Daniel Tchiotsop, Romain Atangana,  
Valérie Louis-Dorr, Didier Wolf

### ► To cite this version:

Laurent Chanel Djoufack Nkengfack, Daniel Tchiotsop, Romain Atangana, Valérie Louis-Dorr, Didier Wolf. EEG signals analysis for epileptic seizures detection using polynomial transforms, linear discriminant analysis and support vector machines. *Biomedical Signal Processing and Control*, 2020, 62, pp.102141. 10.1016/j.bspc.2020.102141 . hal-02931240

**HAL Id: hal-02931240**

**<https://hal.science/hal-02931240>**

Submitted on 12 Jun 2023

**HAL** is a multi-disciplinary open access archive for the deposit and dissemination of scientific research documents, whether they are published or not. The documents may come from teaching and research institutions in France or abroad, or from public or private research centers.

L'archive ouverte pluridisciplinaire **HAL**, est destinée au dépôt et à la diffusion de documents scientifiques de niveau recherche, publiés ou non, émanant des établissements d'enseignement et de recherche français ou étrangers, des laboratoires publics ou privés.

# EEG signals analysis for epileptic seizures detection using polynomial transforms, linear discriminant analysis and support vector machines

Laurent Chanel Djoufack Nkengfack<sup>a,b,\*</sup>, Daniel Tchiotso<sup>b</sup>, Romain Atangana<sup>a,b</sup>,  
Valérie Louis-Door<sup>c</sup>, Didier Wolf<sup>c</sup>

<sup>a</sup> *Unité de Recherche de Matière Condensée-d'Électronique et de Traitement du Signal (UR-MACETS), Faculty of Science, University of Dschang, P.O. Box 67-Dschang, Cameroon*

<sup>b</sup> *Unité de Recherche d'Automatique et d'Informatique Appliquée (UR-AIA), IUT-FV of Bandjoun, University of Dschang, P.O. Box 134-Bandjoun, Cameroon*

<sup>c</sup> *Centre de Recherche en Automatique de Nancy (CRAN), UMR CNRS 7039, ENSEM de Lorraine, Nancy, France*

Electroencephalogram (EEG) signals are useful in understanding the human brain diseases like epilepsy which is characterized by an enduring predisposition to generate epileptic seizures and by neurologic, cognitive, psy-chological and social consequences of these conditions. That is why this paper proposed a novel full processing chain of EEG signals analysis for epileptic seizures detection that applied a new alternative approach for EEG rhythms decomposition. EEG signals are decomposed into their different background rhythms using discrete Jacobi polynomial transforms (JPTs) and a 28-dimension feature vector is extracted in frequency and time do-mains. Due to the high dimension and redundancy of these features, the linear discriminant analysis (LDA) is applied for dimensionality reduction and informative and discriminative low dimension feature vectors are computed and feed as inputs of the support vector machines (SVM) classifiers. The validation of this processing chain is done experimentally using an online available database which consists of five hundred EEG signals. Analysis demonstrated that the EEG rhythms decomposition using JPTs can be implemented as a single-step process and provides more abundant information for class discrimination. In addition, twelve experiments closely related to clinical applications are examined and promising results are achieved with maximum accuracies between 96.25–100 %. Overall, it is found that the proposed processing chain will be useful in providing an accurate and objective scheme for automatic EEG rhythms decomposition and epileptic seizures detection that can be integrated into implantable devices intended to predict the onset of seizures and trigger a focal treatment to block the seizures progression.

## 1. Introduction

Epilepsy is increasingly recognized as a major public health issue since the detection of seizures in epilepsy is a topic of much concern, and his major problem is the diagnosis accuracy [1]. Despite the advent of modern neuroimaging techniques like positron emission tomography (PET), magnetic resonance imaging (MRI) and single photon emission computed tomography (SPECT), the use of electroencephalogram (EEG) signals for epilepsy diagnosis is still convenient. The human EEG is basically non-linear and non-stationary, and may contain useful information about the brain state [2]. However, it is very difficult to get these

useful information directly from these signals by visual inspection since their analysis requires an expert, and is a tedious and time consuming task that can be prone to errors due to fatigue. Hence, efficient EEG signal representation and automatic analysis for time processing reduction, discriminative feature extraction and suitable diagnosis in epilepsy becomes very important.

During these last few decades, many new therapies are being investigated in epilepsy diagnosis and implantable integrated devices that can identify epileptic seizure onset and deliver a direct treatment to affected areas of the brain aims to be the most promising [4–10]. Among many others, Muhammad Tariqus et al. proposed a novel implantable

\* Corresponding author at: Unité de Recherche de Matière Condensée-d'Électronique et de Traitement du Signal (UR-MACETS), Faculty of Science, University of Dschang, P.O. Box 67-Dschang, Cameroon. Tel.: +237 696 11 74 07.

*E-mail addresses:* laurentdjoufack@gmail.com, laurentdjoufack@yahoo.com (L.C. Djoufack Nkengfack), daniel.tchiotso@gmail.com (D. Tchiotso), azongmeromain@gmail.com (R. Atangana), Valerie.Louis@univ-lorraine.fr (V. Louis-Door), Didier.Wolf@univ-lorraine.fr (D. Wolf).

low-power integrated circuit for real-time epileptic seizures detection that was validated in Matlab and gained satisfactory performance with an average seizures detection delay of 13.5 s, well before the onset of clinical manifestations [4]. Wei-Ming et al. also developed an 8-channel closed-loop neural-prosthetic SoC for real-time intracranial EEG (iEEG) acquisition, seizures detection, and electrical stimulation that extracted time-domain entropy and frequency spectrum features, and achieved high detection accuracy of 92 % within 0.8 s [7]. In [9], Muhammad Awais et al. also proposed a non-linear support vector machine (NL-SVM) seizures classification SoC with 8-channel EEG data acquisition and storage for epileptic patients that integrates a feature extraction (FE) engine and patient specific hardware-efficient NL-SVM classification engine which results in an average detection rate, average false alarm rate and latency of 95.1 %, 0.94 % and 2 s, respectively. Otherwise, knowing that these treatments extremely depend on robust systems for seizures detection to perform effectively, more efforts have been also focused only on the development of robust computational models for analysis and automatic detection of epileptic seizures, which then can be integrated into implantable devices. These models generally include a rhythms decomposition stage to determine the optimal features and classifiers. The useful wavelet transform (WT) with different mother wavelet functions [2,3,11–19] and its derivative like tunable-Q WT [20], the empirical mode decomposition (EMD) [21–25], Fourier transform (FT) [26], independent component analysis (ICA) [27], Hilbert-Huang transform (HHT) [28] and Hilbert vibration decomposition (HVD) [29] are extremely applied for the rhythms decomposition process. However, some of these methods do not relate the decomposed rhythms to the ones defined in the literature in terms of spectral coefficients. Also, feature extraction methods are abundantly developed and applied in EEG signals since relevant extracted features improve the performance of the classifier machines. In this impetus, Sutrisno et al. [16] proposed a model based on WT, linear features like standard deviation and band power, non-linear features like Shannon entropy and largest Lyapunov exponent, and classifiers as artificial neural network (ANN), k-nearest neighbor (KNN), SVM and linear discriminant analysis (LDA) which achieves an overall accuracy of 100 % on a healthy versus epileptic seizures detection experiment. Pushpendra et al. [26] used a filter bank signal processing and FT to extract mean frequencies and root mean square bandwidth features as inputs of a least-square SVM (LS-SVM) which gained a maximum accuracy of 100 %. In [27], Sivasankari and Thanushkodi proposed a model that uses the fast ICA and backpropagation neural network for achieving epileptic seizures detection with an overall accuracy of 76.50 % and 66 % for seizure and healthy EEG signals, respectively. Ali Yener [29] also proposed a framework based on HVD and employs estimated instantaneous frequency of largest energy components as features given to LS-SVM for recognizing epileptic seizures with a classification accuracy of 97.66 %.

From the literature, it is firstly observed that most of the reported models have a limited success rate. In addition, some models extend to be very complex for practical applications, and other models used high dimension features that are not easily viewed and interpreted, and generally are not sufficiently representative and discriminative for the EEG signal classification. On the other hand, most of the reported models did not select their parameters using a suitable technique, although the parameters significantly affect the classification performance. In short, to the best of our knowledge and in spite of many techniques used, polynomial transforms are not yet exhaustively applied for the purpose of epilepsy diagnosis even if the physical interpretation of the spectral coefficients could also establish correlations with some pathologies, leading to a new issue for automatic diagnosis and seizures detection [30]. Also, in line with optimal smoothing, it is demonstrated that modeling remains an important technique for time series analysis (information retrieval, noise removal from measurements and feature extraction for pattern classification problems) in which a mathematical model is fitted to a sampled signal [31–34]. That is why this paper proposed a novel full processing chain of EEG signals analysis for

epileptic seizures detection that applied a new alternative approach based on polynomial transforms for EEG rhythms decomposition. With this intention, Jacobi polynomial transforms (JPTs) namely discrete Legendre transform (DLT) and discrete Chebychev transform (DChT) are derived to explore EEG signals in the frequency domain. EEG data are projected into a set of spectral coefficients, and low dimension and discriminative features are extracted using LDA and feed as inputs of SVM classifiers for epileptic seizures detection.

The rest of this paper is organized as follows. In Section 2, we briefly present EEG data sets and some properties of Jacobi polynomials which help to construct the modelling scheme of sampled data via Legendre and Chebychev polynomials. The full processing chain for EEG seizures detection is described and includes the rhythms decomposition, feature extraction, dimensionality reduction using LDA, and SVM classifiers steps. Twelve experiments closely related to clinical applications are examined for the test of the proposed full processing chain. In Section 3, simulation results are presented and discussed. Then, the conclusion and some perspectives are presented in the last section.

## 2. Materials and methodology

This section described the materials used and the proposed full processing chain of EEG signals analysis for seizures detection. This proposed processing chain includes some stages (EEG signal acquisition, EEG analysis and classification) and few steps that are depicted in Fig. 1 and briefly described in the following sub-sections.

### 2.1. Data description

The data consists of five sets (SET A-E) of EEG signals [35]. Each set contains 100 EEG derivations recording with the sampling frequency of 173.61 Hz and resulting to a 86.805 Hz bandwidth with respect to the Nyquist theorem. SETS A (Z001 to Z100) and B (O001 to O100) consist of data collected from five healthy volunteers in an awake state with eyes opened and closed using scalp electrodes, respectively. SETS C (N001 to N100) and D (F001 to F100) derivations have been measured in seizure-free intervals from five patients within the hippocampal formation of the opposite hemisphere of the brain and within the epileptogenic zone, respectively. SET E (S001 to S100) consists of data recorded during a seizure. SETS C, D and E data have been acquired intracranially. The duration of each segment is 23.6 s, which leads to 4097 samples. Fig. 2 presents an example of EEG signals of the data.

### 2.2. Jacobi polynomial transforms (JPTs)

#### 2.2.1. Jacobi polynomials

Jacobi polynomials are one of the great classes of orthogonal polynomials that have very interesting properties, which makes them very attractive for an optimal polynomial interpolation [36–38]. They are orthogonal on the interval  $[-1, 1]$  with respect to the weight function  $\omega(x) = (1-x)^\alpha(1+x)^\beta$ , with  $\alpha, \beta > -1$ .

The continuous orthogonality condition is expressed by:

$$\langle J_i^{\alpha,\beta}, J_j^{\alpha,\beta} \rangle_\omega = \int_{-1}^1 J_i^{\alpha,\beta}(x) J_j^{\alpha,\beta}(x) (1-x)^\alpha (1+x)^\beta dx = C_i^2 \delta_{ij} \quad (1)$$

Where  $C_i = \|J_i^{\alpha,\beta}\|_{L_\omega^2}$  and  $\delta_{ij}$  is the Kronecker symbol given by  $\delta_{ij} =$

$$\begin{cases} 1, & i = j \\ 0, & i \neq j \end{cases}$$

Discrete Jacobi polynomials satisfy the discrete orthogonality relation expressed by:

$$\langle J_i^{\alpha,\beta}, J_j^{\alpha,\beta} \rangle_\omega = \sum_{k=0}^L J_i^{\alpha,\beta}(x_k) J_j^{\alpha,\beta}(x_k) (1-x_k)^\alpha (1+x_k)^\beta = C_{ij}^2 \delta_{ij} \quad (2)$$

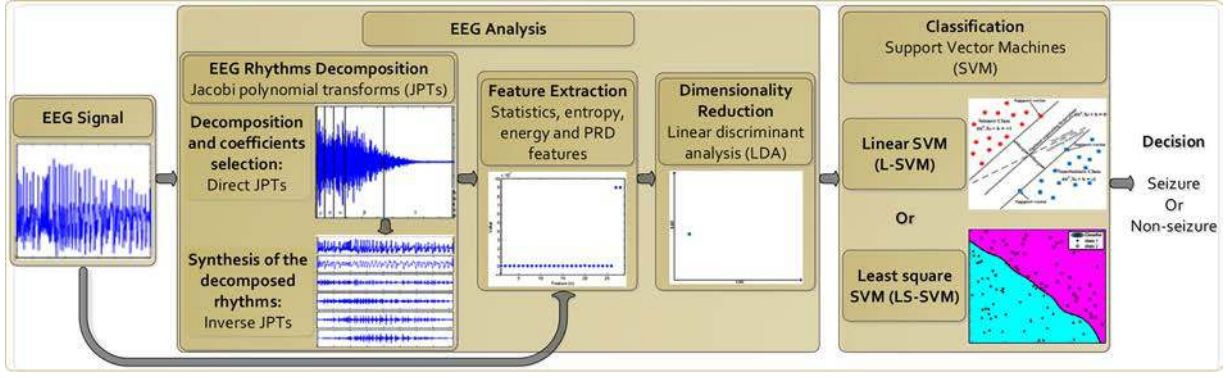


Fig. 1. Full processing chain of EEG signals analysis for seizures detection.

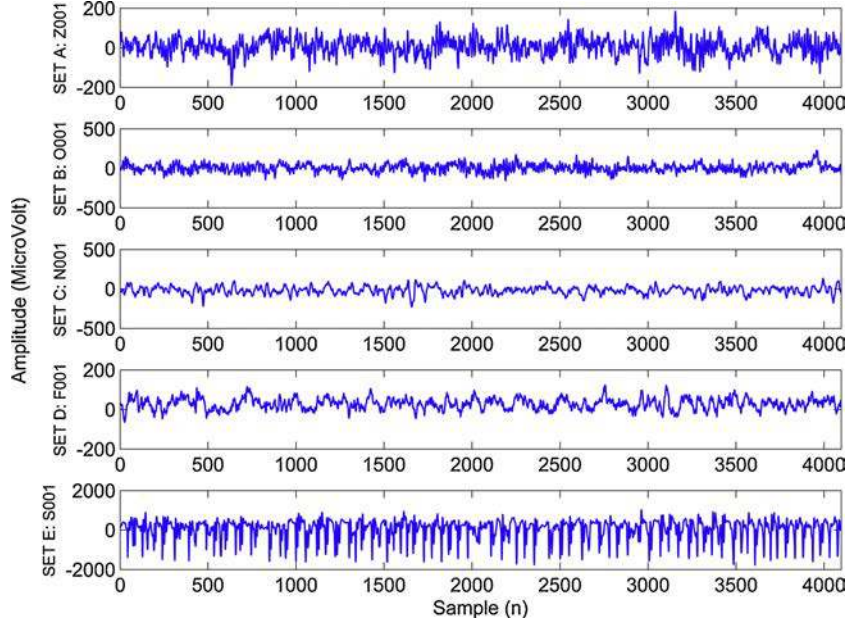


Fig. 2. Examples of EEG signals. From top to bottom: SET A Healthy EEG Z001, SET B Healthy EEG O001, SET C Seizure-free EEG N001, SET D Seizure-free EEG F001 and SET E Seizure EEG S001 [35].

In the same way, Jacobi polynomials satisfy the differential equation and the Rodrigue formula defined by Eqs. (3) and (4), respectively:

$$(1-x)^{-\alpha}(1+x)^{-\beta} \frac{d}{dx} \left\{ (1-x)^{\alpha+1}(1+x)^{\beta+1} \frac{d}{dx} J_i^{\alpha,\beta}(x) \right\} + i(i+1+\alpha + \beta) J_i^{\alpha,\beta}(x) = 0, \quad i \geq 0 \quad (3)$$

$$(1-x)^\alpha(1+x)^\beta J_i^{\alpha,\beta}(x) = \frac{(-1)^i}{2^i i!} \frac{d^i}{dx^i} [(1-x)^{i+\alpha}(1+x)^{i+\beta}], \quad i \geq 0 \quad (4)$$

In this paper, we focus on two special cases of Jacobi polynomials namely Legendre polynomials and Chebychev polynomials of the 1<sup>st</sup> kind, with some properties presented in the Appendix.

### 2.2.2. Polynomial expansion

The polynomial expansion of a signal  $s(x)$  to an order "M" in the orthogonal Jacobi base is a function given by:

$$s(x) = \sum_{k=0}^M \alpha_k J_k^{\alpha,\beta}(x) \quad (5)$$

Where the sequence of coefficients  $\{\alpha_k\}_{k=0}^M$  constitutes the spectral coefficients of decomposition or projection of the signal  $s$  in the Jacobi

polynomial base and are evaluated by:

$$\alpha_k = \frac{\int_{-1}^1 s(x) J_k^{\alpha,\beta}(x) \omega(x) dx}{\int_{-1}^1 J_k^{\alpha,\beta}(x) J_k^{\alpha,\beta}(x) \omega(x) dx} = \frac{1}{d_k^2} \int_{-1}^1 s(x) J_k^{\alpha,\beta}(x) \omega(x) dx \quad (6)$$

$$\text{With } d_k^2 = |J_k^{\alpha,\beta}|^2 = \int_{-1}^1 J_k^{\alpha,\beta}(x) J_k^{\alpha,\beta}(x) \omega(x) dx$$

The evaluation of the coefficients  $\alpha_k$  is done efficiently with the Gauss-Lobatto method. Gauss-Labatto method is a powerful tool for numerical integrations, especially dedicated to orthogonal polynomials [36]. In short, the Gauss quadrature's stipulates that for a family of orthogonal polynomials  $\{P_k(x)\}$  in the interval  $[a, b]$ , with respect to the weight function  $\omega(x)$ , the following approximation is done:

$$\int_a^b f(x) \omega(x) dx \approx \sum_{j=0}^M G_j f(x_j) \quad (7)$$

Where  $f(x) \in L^2[a, b]$ ,  $x_j$  are the  $M+1$  nodes of  $P_{M+1}(x)$  and  $G_j$  are the Gauss coefficients or weights called "Christoffel numbers".

### 2.2.3. Discrete Legendre transform (DLT)

For Legendre polynomials, Eqs. (5) and (6) become, respectively:

$$s(x) = \sum_{k=0}^M \alpha_k L_k(x) \quad (8)$$

$$\alpha_k = \frac{\langle s(x), L_k(x) \rangle}{\langle L_k(x), L_k(x) \rangle} = \frac{\langle s, L_k \rangle}{\langle L_k, L_k \rangle} = \frac{\int_{-1}^1 s(x) L_k(x) dx}{\int_{-1}^1 L_k^2(x) dx} = \frac{1}{d_k^2} \int_{-1}^1 s(x) L_k(x) dx \quad (9)$$

With  $d_k^2$  given by Eq. (A.2), and the application of the Gauss-Lobatto method gives:

$$\int_{-1}^1 s(x) L_k(x) dx = \frac{2}{M(M+1)} \sum_{j=0}^M \frac{s(x_j) L_k(x_j)}{[L_M(x_j)]^2} \quad (10)$$

Where  $x_j$  are the  $M+1$  Gauss-Lobatto nodes of  $(1-x^2)L'_M(x)$  formed by  $x_0 = -1$ ,  $x_M = 1$  and  $x_j$  nodes of  $L'_M(x)$ ,  $j = 1, 2, \dots, M-1$  computed using the eigenvalue method described in [38]. Christoffel numbers are given by  $G_j = \frac{2}{M(M+1)} \frac{1}{[L_M(x_j)]^2}$ ,  $j = 0, 1, 2, \dots, M$ .

Then, the DLT is expressed as follows:

$$\left\{ \begin{array}{l} \alpha_k = \frac{2k+1}{M(M+1)} \sum_{j=0}^M \frac{L_k(x_j)}{[L_M(x_j)]^2} s(x_j), \quad k = 0, 1, \dots, M-1 \\ \alpha_M = \frac{1}{M+1} \sum_{j=0}^M \frac{s(x_j)}{L_M(x_j)}, \quad k = M \end{array} \right. \quad (11)$$

### 2.2.4. Discrete Chebychev transform (DChT)

For Chebychev polynomials, Eqs. (5) and (6) become, respectively:

$$s(x) = \sum_{k=0}^M \alpha_k T_k(x) \quad (12)$$

$$\alpha_k = \frac{\langle s(x), T_k(x) \rangle}{\langle T_k(x), T_k(x) \rangle} = \frac{\langle s, T_k \rangle}{\langle T_k, T_k \rangle} = \frac{\int_{-1}^1 \frac{s(x) T_k(x)}{\sqrt{1-x^2}} dx}{\int_{-1}^1 \frac{T_k^2(x)}{\sqrt{1-x^2}} dx} = \frac{1}{d_k^2} \int_{-1}^1 \frac{s(x) T_k(x)}{\sqrt{1-x^2}} dx \quad (13)$$

With  $d_k^2$  given by Eq. (A.5), and the application of the Gauss-Lobatto method gives:

$$\int_{-1}^1 \frac{s(x) T_k(x)}{\sqrt{1-x^2}} dx = \frac{\pi}{M+1} \sum_{j=0}^M s(x_j) T_k(x_j) \quad (14)$$

Where  $x_j$  are the  $M+1$  zeros of  $T_{M+1}(x)$  given by Eq. (A.7). All Christoffel numbers are equal to  $G_j = \frac{\pi}{M+1}$ ,  $j = 0, 1, 2, \dots, M$ .

Then, the DChT is expressed as follows:

$$\left\{ \begin{array}{l} \alpha_0 = \frac{1}{M+1} \sum_{j=1}^{M+1} s(x_j) = \frac{1}{M+1} \sum_{j=1}^{M+1} s \left\{ \cos \left[ \frac{(2j-1)}{2(M+1)} \pi \right] \right\} \\ \alpha_k = \frac{2}{M+1} \sum_{j=1}^{M+1} s(x_j) \cos \left[ \frac{k(2j-1)}{2(M+1)} \pi \right] \\ = \frac{2}{M+1} \sum_{j=1}^{M+1} s \left\{ \cos \left[ \frac{(2j-1)}{2(M+1)} \pi \right] \right\} * \cos \left[ \frac{k(2j-1)}{2(M+1)} \pi \right], \quad k = 1, 2, 3, \dots, M \end{array} \right. \quad (15)$$

## 2.3. EEG analysis

### 2.3.1. EEG rhythms decomposition using JPTs

The uneven distribution of the signal energy in the frequency domain has made the physical interpretation of the spectral coefficients after decomposition an important practical problem. This sub-section presents a new alternative approach for the efficient and instantaneous decomposition of the EEG rhythms. This approach is based on the projection of the EEG signals into polynomial bases, which lead to polynomial interpolation. Knowing that the five primary EEG rhythms called delta (0.5–4 Hz), theta (4–8 Hz), alpha (8–13 Hz), beta (13–30 Hz), and gamma (30–60 Hz) generally span the 0.5–60 Hz frequency range and higher frequencies are often characterized as noise, this approach includes some few steps that are depicted in Fig. 3 and briefly described in the following.

- The current EEG signal,  $t \in [0, t_B]$  is of finite energy and can be decomposed in the Jacobi polynomial base. It should be transposed into  $[-1, 1]$  domain by a simple linear transformation  $x = -1 + 2t/t_B$ .
- The order of decomposition is chosen such that the percent root square difference (PRD) is lower than 7 % and the quasi-totality of the original signal information is conserved after decomposition [39]. For an automatic detection of epileptic states, the maximum acceptable PRD is equal to 30 % [30,40]. Sometimes, certain roots of Jacobi polynomials are not images of signal samples within the interval  $[-1, 1]$ , in these cases,  $S(x_j)$  is calculated using the spline cubic interpolation function.
- The selection of coefficients used to synthesize each EEG rhythm is based on the FT. The fast FT is applied to discrete Jacobi polynomials and their energy spectral density (ESD) is computed. The frequency with the maximum ESD is used as parameter for the selection of corresponding spectral coefficients of each EEG rhythm, and the other spectral coefficients correspond to noise.

$$ESD(f) = |X(f)|^2 \quad (16)$$

Where  $X(f) = DFT\{x(k)\}$

- Therefore, using the corresponding spectral coefficients for reconstruction through Eq. (5) provides the rhythms decomposition of the EEG signal.

### 2.3.2. Feature extraction

The main aim of feature extraction is to obtain further information from the raw signal by transforming the large data into a fewer feature vector. After processing the data with the JPTs, feature extraction methodology analyzes signals to extract the most prominent features that are representative of the various classes of signals. Then, the time and frequency distribution of the EEG signal can be represented by typical statistical, entropy and energy features [41]:

- Maximum (Max) of the absolute values of the spectral coefficients in each EEG rhythm.
- Mean of the absolute values of the spectral coefficients in each EEG rhythm.
- Standard deviation (Std1) of the spectral coefficients in each EEG rhythm.
- Standard deviation (Std2) of the absolute values of the spectral coefficients in each EEG rhythm.
- Entropy (S) of the absolute values of the spectral coefficients in each EEG rhythm. For the EEG rhythm with spectral coefficients  $\alpha_j$ , it is expressed by:

$$S = \sum_k |\alpha_j(k)| * \log(|\alpha_j(k)|^2) \quad (17)$$

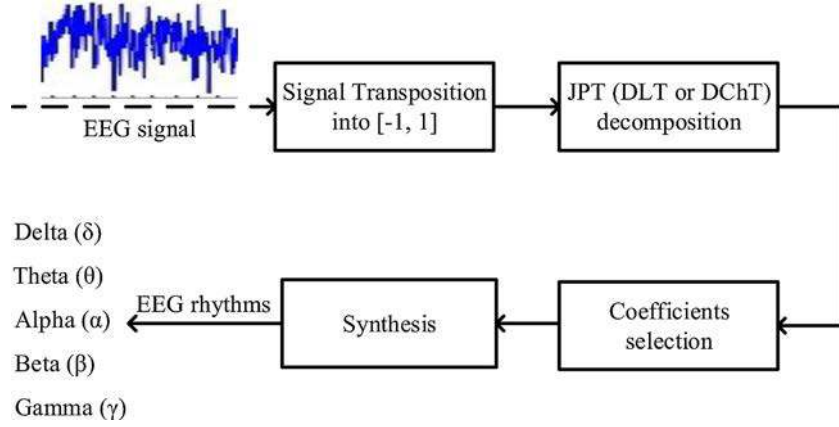


Fig. 3. Approach of EEG rhythms decomposition using JPTs.

- Energy of the original EEG signal ( $E$ ).
- Energy of the approximate EEG signal ( $E_{app}$ ).
- Percent root square difference (PRD) of the EEG signal. For the EEG signal  $\{s_n\}_{n=1,2,\dots}$  and the approximate ones  $\{\tilde{s}_n\}_{n=1,2,\dots}$ , PRD is expressed by:

$$PRD (\%) = 100 \sqrt{\frac{\sum_n (s_n - \tilde{s}_n)^2}{\sum_n s_n^2}} \quad (18)$$

### 2.3.3. Dimensionality reduction using linear discriminant analysis (LDA)

In machine learning, the desired goal of dimensionality reduction is to decrease the dimension of a  $d$ -dimensional data by projecting it onto a  $k$ -dimensional subspace (where  $k \leq d$ ). This is done in order to increase the computational efficiency while reducing information noise and redundancy, and retaining most of the relevant information about the original data.

In this paper, we applied LDA also called Fisher's discriminant analysis for dimensionality reduction. LDA is a supervised algorithm that computes the linear discriminant by maximizing the distance between classes and minimizing the distance within classes [42]. At the end of the procedure, each class will have a normal distribution of discriminant parameters. The projection can be written as a single matrix equation given by:

$$Y = X * W \quad (19)$$

Where  $Y$  and  $X$  are new and old features, respectively.  $W$  is the  $dxk$  projection matrix formed by the first  $k$ -eigenvectors of  $S_w^{-1}S_b$ , where  $S_w$  and  $S_b$  are the within-class and between-class scatter matrices, respectively.

$$S_w = \frac{1}{N} \sum_{l=1}^L \sum_{i=1}^{N_l} (x_i^l - \mu_l)^T (x_i^l - \mu_l) \quad (20)$$

$$S_b = \frac{1}{N} \sum_{l=1}^L N_l (\mu_l - \mu)^T (\mu_l - \mu) \quad (21)$$

$x_i^l$ ,  $N_l$  and  $\mu_l$  are an  $i$ -row vector, the number of  $i$ -vectors and the mean vector corresponding to class label  $l$ , respectively.  $L$ ,  $N$  and  $\mu$  are the number of classes, the total number of  $i$ -vectors and the global mean of all classes, respectively.

## 2.4. Classification

### 2.4.1. Linear support vector machine (L-SVM)

Introduced by Vapnik [43], SVM is a popular, discriminative and

supervised binary machine learning algorithm defined by an optimal separating hyperplane. L-SVM learns a given training dataset  $\{(x_k, y_k)\}_{k=1}^N$  with input  $x_k \in \mathbb{R}^n$  and output label  $y_k \in \{+1, -1\}$  that forms the binary classes. The support vector classifier chooses one particular solution, the classifier that separates the classes with maximal margin  $m$ , as seen in Fig. 4. This linear classifier  $\omega^T X + b = 0$  must generalize well on unseen examples. The goal is to classify EEG signals for epileptic seizures detection using 1- and 2-dimension linear functions which are induced from available examples.

### 2.4.2. Least-square support vector machine (LS-SVM)

LS-SVM is a least square extension of the SVM classifier introduced by Suykens and Vandewalle [44]. The formulation of the LS-SVM classifier leads to solving a set of linear equations, instead of quadratic programming for classical SVM. This is due to equality constraints defined by Eq. (22). The LS-SVM parameters'  $\omega = \sum_{k=1}^N \alpha_k \gamma_k \varphi(x_k)$  and  $b$  are solutions of the dual problem derived by Eqs. (22) and (23).

$$y_k [\omega^T \varphi(x_k) + b] = 1 - \varepsilon_k \quad , \quad k = 1, 2, \dots, N \quad (22)$$

$$\min_{\omega, b, \varepsilon} J(\omega, b, \varepsilon) = \frac{1}{2} \omega^T \omega + \frac{1}{2} \gamma \sum_{k=1}^N \varepsilon_k^2 \quad (23)$$

Where  $\{(x_k, y_k)\}_{k=1}^N$ ,  $\gamma$  and  $\varepsilon_k, k=1,2,\dots,N$  represent the training set with input  $x_k \in \mathbb{R}^n$  and output label  $y_k \in \{+1, -1\}$ , the regularization parameter and the errors between the desired and the obtained outputs

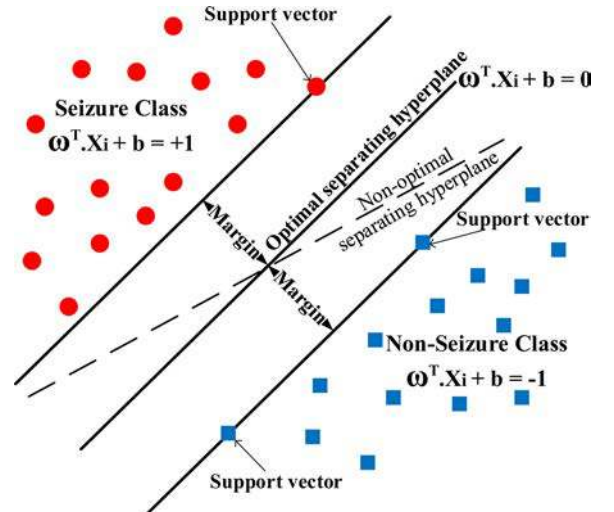


Fig. 4. Optimal linear separating hyperplane.

of the LS-SVM, respectively.

The Lagrangian for the problem is:

$$L(\omega, b, \varepsilon; \alpha) = J(\omega, b, \varepsilon) - \sum_{k=1}^N \alpha_k \{ y_k [\omega^T \varphi(x_k) + b] - 1 + \varepsilon_k \} \quad (24)$$

Where  $\alpha_k, k=1,2,\dots,N$  are the Lagrange multipliers, and the condition for optimality yield to:

$$\begin{cases} \frac{\partial L}{\partial \omega} = 0 \rightarrow \omega = \sum_{k=1}^N \alpha_k y_k \varphi(x_k) \\ \frac{\partial L}{\partial b} = 0 \rightarrow \sum_{k=1}^N \alpha_k y_k = 0 \\ \frac{\partial L}{\partial \varepsilon_k} = 0 \rightarrow \alpha_k = \gamma \varepsilon_k, \quad k = 1, 2, \dots, N \\ \frac{\partial L}{\partial \alpha_k} = 0 \rightarrow y_k [\omega^T \varphi(x_k) + b] - 1 + \varepsilon_k = 0, \quad k = 1, 2, \dots, N \end{cases} \quad (25)$$

Defining  $Y = [y_1, y_2, \dots, y_N]^T, \bar{1} = [1, 1, \dots, 1]^T, \varepsilon = [\varepsilon_1, \varepsilon_2, \dots, \varepsilon_N]^T, \alpha = [\alpha_1, \alpha_2, \dots, \alpha_N]^T$ , the identity matrix  $I$ , and  $\Omega_{kl} = y_k y_l \varphi(x_k)^T \varphi(x_l) = y_k y_l K(x_k, x_l)$  by applying Mercer's conditions for kernels, the following linear system is obtained.

$$\begin{bmatrix} 0 & Y^T \\ Y & \Omega + \gamma^{-1} I \end{bmatrix} \begin{bmatrix} b \\ \alpha \end{bmatrix} = \begin{bmatrix} 0 \\ \bar{1} \end{bmatrix} \quad (26)$$

Then, the LS-SVM classifier in the dual space takes the form:

$$y(x) = \text{sign}[\omega^T \varphi(x_k) + b] = \text{sign} \left[ \sum_{k=1}^N \alpha_k y_k K(x, x_k) + b \right] \quad (27)$$

#### 2.4.3. Design of experiments

Twelve classification experiments are elaborated from the above data and summarizes in Table 1. These experiments are closely related to clinically relevant applications as well as their wide usage by various researchers for EEG signals classification, and can permit to compare the performance of the proposed full processing chain to other ones.

- In the first, second, third and fourth experiments, healthy versus seizure, and seizure-free versus seizure are examined. The non-seizure class includes SET A, SET B, SET C or SET D, respectively, while the seizure class includes SET E which forms the EEGs data recorded during epileptic seizures.
- In the fifth and sixth experiments, healthy versus seizure and seizure-free versus seizure are examined, respectively. The non-seizure class includes SETs A-B or SETs C-D, while the seizure class includes SET E.
- In the seventh and eighth experiments, SETs A-C-D and SETs A-B-C-D form the non-seizure classes, respectively, while SET E forms the seizure class.
- In the ninth and tenth experiments, healthy versus seizure-free and healthy versus seizure-free + seizure are examined, respectively. SETs A-B form the non-seizure class while SETs C-D and SETs C-D-E form the seizure class, respectively.
- In the eleventh experiment, healthy EEG with eyes opened and eyes closed are discriminated into two different classes.
- In the twelfth experiment, all the EEGs from the data are used and discriminated into three different classes. For this multiclass, the one versus the rest strategy is used and consists in separating each class from all the others. To address this three-class experiment, we combine two binary (two-class) experiments, ABCD-E / AB-CD and AB-CDE / CD-E.

#### 2.4.4. Metrics for performance evaluation

The performance of the full processing chain for seizures detection is evaluated using three metrics namely specificity, sensitivity and accuracy. These metrics are defined as [42]:

**Table 1**

Classes and corresponding number of EEG derivations for twelve classification experiments. HF and EZ stand to hippocampal formation and epileptogenic zone, respectively.

Experiment	Classes	Number of EEG derivations
A - E	Healthy with eyes opened - Seizure	100 - 100
B - E	Healthy with eyes closed - Seizure	100 - 100
C - E	Seizure-free within the HF - Seizure	100 - 100
D - E	Seizure-free within the EZ - Seizure	100 - 100
AB - E	Healthy - Seizure	200 - 100
CD - E	Seizure-free - Seizure	200 - 100
ACD - E	Healthy with eyes opened + Seizure-free - Seizure	300 - 100
ABCD - E	Healthy + Seizure-free - Seizure	400 - 100
AB - CD	Healthy - Seizure-free	200 - 200
AB - CDE	Healthy - Seizure-free + Seizure	200 - 300
A - B	Healthy with eyes opened - Healthy with eyes closed	100 - 100
AB - CD - E	Healthy - Seizure-free - Seizure	200 - 200 - 100

- **Specificity (SPE):** Total number of correctly detected negative patterns ( $TN_{CN}$ ) / Total number of actual negative patterns ( $TN_{AN}$ ). A negative pattern indicates a non-seizure EEG.

$$SPE (\%) = 100 * \frac{TN_{CN}}{TN_{AN}} \quad (28)$$

- **Sensitivity (SEN):** Total number of correctly detected positive patterns ( $TN_{CP}$ ) / Total number of actual positive patterns ( $TN_{AP}$ ). A positive pattern indicates a seizure EEG.

$$SEN (\%) = 100 * \frac{TN_{CP}}{TN_{AP}} \quad (29)$$

- **Accuracy (ACC):** Total number of correctly classified patterns ( $TN_{CP} + TN_{CN}$ ) / Total number of patterns ( $TN_{AP} + TN_{AN}$ ).

$$ACC (\%) = 100 * \frac{TN_{CN} + TN_{CP}}{TN_{AN} + TN_{AP}} \quad (30)$$

#### 2.5. Proposed full processing chain description

A novel full processing chain of EEG signals analysis for epileptic seizures detection that applied a new alternative approach for EEG rhythms decomposition is proposed and presented in Fig. 1. This processing chain includes three major stages that are EEG signal acquisition, EEG analysis, and classification. At the signal acquisition stage, we used an online available database which consists of five hundred EEG signals divided into five different classes. After signal acquisition, the EEG are analyzed at the second stage according to three steps namely EEG rhythms decomposition, feature extraction and dimensionality reduction, respectively. The efficient and instantaneous decomposition of the EEG rhythms is based on the projection of the EEG signals into Jacobi polynomial bases using JPTs namely DLT and DChT. Furthermore, we analyze the original signals and theirs corresponding rhythms in terms of statistical, energy and entropy features, and a 28-dimension feature vector is extracted in frequency and time domains. Due to the high dimension and redundancy of the extracted features, and in order to improve the discriminative properties of the signals of various classes, the LDA is applied for dimensionality reduction and new informative and discriminative low dimension feature vectors are computed. At the last stage of the proposed processing chain, the 1- and 2-dimension feature vectors are then classified either with L-SVM or LS-SVM with Gaussian radial basis function (RBF) kernel  $K(x, x_k) = \exp\left(-\frac{1}{2\sigma^2} \|x_k - x\|^2\right)$  such that a decision can be taken as seizure or non-seizure.

For dimensionality reduction and classification, the 60 % of each SET are used to form the training set and the other 40 % are used to form the testing set. The training set is required to construct the model while the testing set is required to estimate the model performance. This work used the LS-SVM toolbox proposed in [45] where the *tunlssvm* function with 5-fold cross validation technique and the *trainlssvm* function are used to find the regularization and kernel parameter (*gam*, *sig2*) of the optimal LS-SVM classifier. Therefore, the *simlssvm* function is used to determine the performances of the optimal LS-SVM classifier.

What is new is the alternative approach which consists of applying JPTs for the rhythms decomposition. This is important because the physical interpretation of the spectral coefficients could establish correlations with epileptic seizures. Also, discriminative low dimension features that are easily viewed, sufficiently representative and interpreted are extracted instead of high dimension features such that the classification performance can be significantly improved. Overall, the proposed processing chain extends to be less complex for practical applications and it will be useful to clinicians in providing an accurate and objective scheme in epileptic seizures detection and prediction.

### 3. Results and discussion

This section presents the experimental outcomes of the proposed approach for EEG rhythms decomposition, feature extraction, dimensionality reduction and epileptic seizures detection. All experiments are carried out using MATLAB (version 8.1, R2013a) on a HP EliteBook Folio 9470m-Intel(R) Core(TM) i5-3437U with 2.40 GHz, 8.00 Go RAM and Windows 10. This section also provides a comparison between the proposed processing chain and other well-known existing ones.

#### 3.1. Results of EEG rhythms decomposition and feature extraction

EEG signals are interpolated and their frequency distributions are represented by typical statistical, entropy and energy features that are representative of the various classes of signals. Fig. 5 presents examples of EEG rhythms decomposition and corresponding  $10^{-5} \cdot \text{ESD}$ .

From the supervision of Fig. 5 it is related that EEG rhythms obtained with DLT and DChT are more correlated. One advantage of this method is that no pre-processing stage is needed because frequency occupation of the approximated signal increases with the degree of the discrete Jacobi polynomials. Then, the proposed method combines the pre-processing and processing stages simultaneously, and the decomposition of EEG rhythms can be implemented as a one-step process. Furthermore, JPTs can gather as well as possible the EEG rhythms by reducing overlapping and eliminating the continuous component.

After processing the data with the JPTs, EEG signal of 4097 samples is transformed into a 28-dimension feature vector. In total, a  $100 \times 28$ -dimension feature vector is extracted for each SET. Figs. 6 and 7 present a comparison of the frequency distribution of each SET in terms of extracted features. Firstly, boxplots of extracted features show that the evolution of each feature presents similarities in different rhythms. It can be seen that, the same information is extracted from the different rhythms. Secondly, E and Eapp features also present similar information for different classes of EEGs. Then, these extracted features are representative for the various classes but still present redundancy. Even though, for direct discrimination, few of these features individually carry discriminative information about their classes.

#### 3.2. Results of dimensionality reduction and seizures detection

Since the extracted feature vectors are not easily viewed and

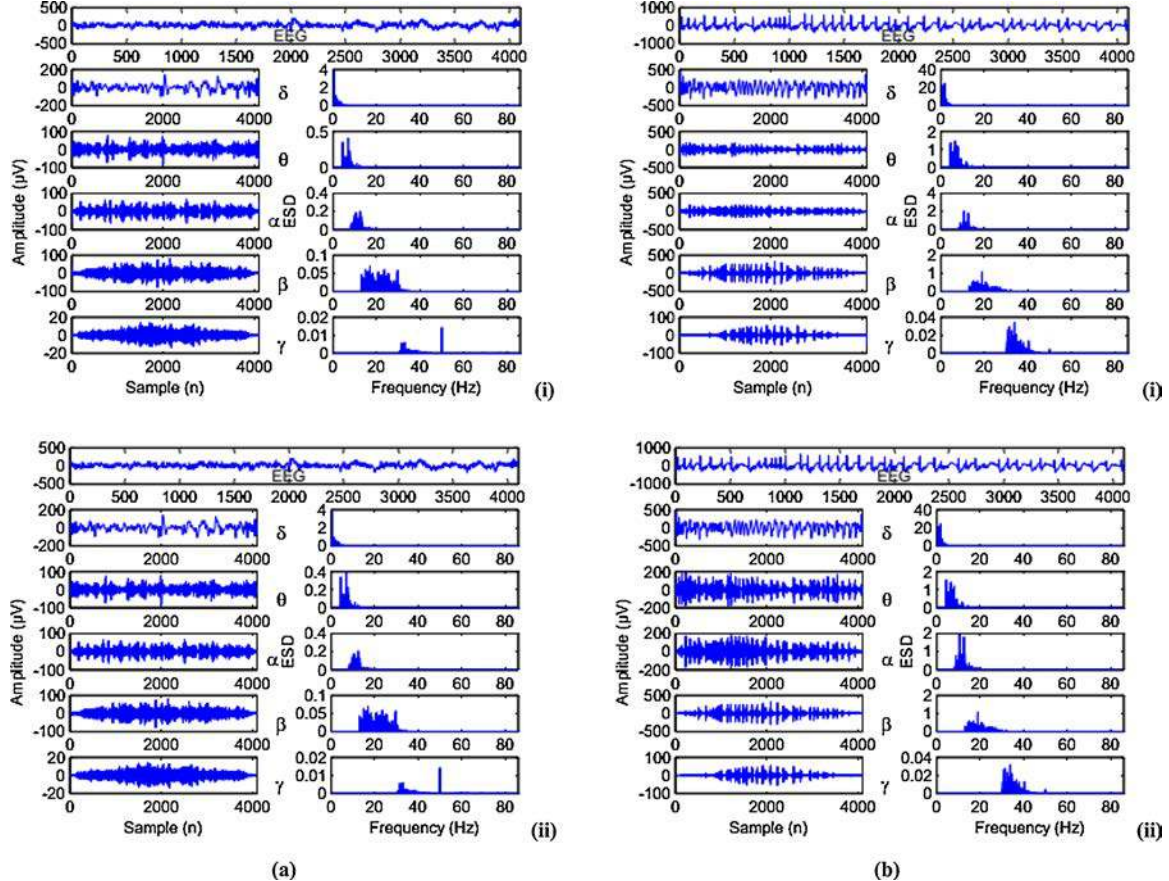


Fig. 5. EEG rhythms decomposition of (a) a healthy EEG Z018 and (b) a seizure EEG S018 using (i) DLT and (ii) DChT.

interpreted, this task of dimensionality reduction is necessary. Therefore, only the first two linear discriminants (LDs) are used to derive our new features subspace since the explained variance tells us that they contain the quasi totality of the information. For each experiment, Figs. 8 and 9 present the comparison of the new features subspace obtained using LDA.

Figs. 8 and 9 present the discriminative effect that exist between classes for different experiments after dimensionality reduction using LDA. It is observed that the computed 1- and 2-dimension features obtained with LDA after JPTs rhythms decomposition are more informative and discriminative for all experiments. In more experiments, the computed low dimension features are less overlapping. On the other hand, LDA tries to explicitly model differences between class labels within the data and successful discrimination for different experiments can be achieved using SVM classifiers like L-SVM and LS-SVM.

Therefore, the 1- and 2-dimension feature vectors are used as benchmarks for the L-SVM and LS-SVM, and the seizures detection accuracies of the twelve experiments are presented in Tables 2 and 3. Then, the highest performances of the twelve experiments are summarized in Table 4.

For each experiment in Table 2, it is clearly observed that obtained L-SVM detection accuracies are higher using the extracted 1-dimension LDA feature vector. DLT and DChT analysis give similar results, except for the ABCD-E, AB-CD and AB-CDE experiments where DLT analysis give better detection accuracies, and for the D-E and A-B experiments where DChT analysis gives higher detection accuracies. For the AB-CD-E multiclass experiment, the L-SVM gather the highest detection accuracy of 99.44 % using the ABCD-E / AB-CD combination in DChT analysis with the extracted 1-dimension LDA feature. For each experiment, Table 3 demonstrates that the LS-SVM classifier gather highest detection accuracies with the extracted 1-dimension feature vectors. In general, JPTs - LDA - LS-SVM models give similar results, except for the D-E, CD-E, ABCD-E, AB-CD and AB-CDE where the DLT analysis gives higher detection accuracies than the DChT analysis. The ABCD-E / AB-CD combination proves to be more accurate than the AB-CDE / CD-E combination for the multiclass experiment.

In general, Table 4 shows that for the A-E, B-E, C-E, D-E, AB-E, CD-E, ACD-E and ABCD-E experiments, JPTs-LDA-SVM fully detect seizures

EEG signals with a highest detection accuracy of 100 %. The extracted 1- and 2-dimension features as inputs of the SVM classifiers can also evaluate the AB-CD and AB-CDE experiments with maximum seizures detection accuracies of 99.38 % and 97.50 %, respectively. For the AB-CD-E multiclass experiment, the SVM classifier gives higher seizures detection accuracy of 99.44 % using ABCD-E / AB-CD combination. The lowest seizures detection accuracy is found to be 96.25 % for the A-B experiment. Overall, it is found that for each experiment, the performances of the SVM classifiers are higher.

### 3.3. Discussion

During these recent years, advancements and refinement of automatic classification systems have led to the ability to detect epileptic seizures. An increasing interest is focus in the development of several automatic classification systems using linear and non-linear methods on temporal, frequency and time-frequency domains. In this impetus, several processing chains have been proposed. For comparison, Table 5 presents more other processing chains that use the same data and different extracted feature vectors for epileptic seizures detection. It is seen that this paper presents a novel processing chain of epileptic seizures detection using JPTs at the EEG rhythms decomposition step.

As it is a problem of first importance, A-E, B-E, C-E and D-E experiments are extremely examined. For this purpose, we present a processing chain which yields highest seizures detection accuracy of 100 % for all these four experiments. These results are better than the seizures detection accuracies obtained by Ocak [12] (99.60 %), and Ling Guo et al. [13] (99.60 %) for the for A-E experiment. However, some works proposed different processing chains and models that extend to perform better. Thus, Sutrisno et al. [16] proposed a processing chain based on WT, linear and non-linear features, and ANN, KNN and SVM classifiers which also achieves an overall accuracy of 100 % for the A-E experiment. Tzallas et al. [46] also proposed a model that realized a time-frequency analysis of EEG signals and used the ANN classifier which gained a seizures detection accuracy of 100 % for the A-E experiment. Furthermore, our processing chain is also better than others in examining two, three or four of these first experiments. In this impetus, Nicolaou et al. [47] proposed a less accurate processing chain

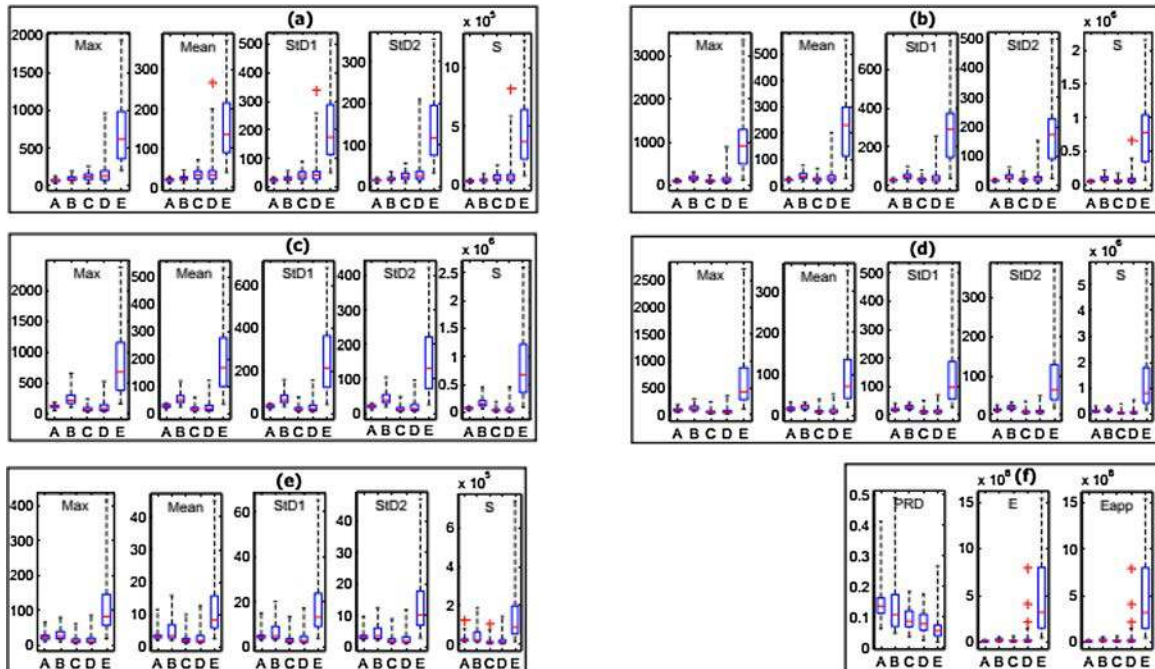


Fig. 6. Comparison of typical statistics, entropy and energy features at the (a) Delta, (b) Theta, (c) Alpha, (d) Beta and (e) Gamma rhythms, and at the (f) EEGs using DLT.

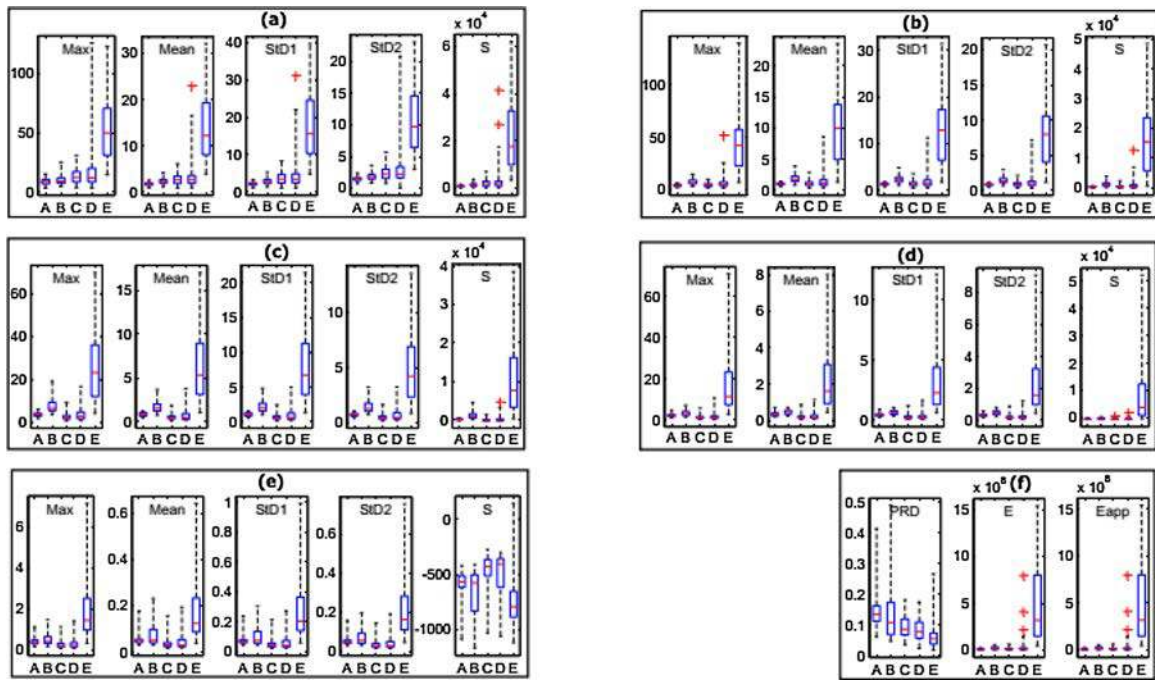


Fig. 7. Comparison of typical statistics, entropy and energy features at the (a) Delta, (b) Theta, (c) Alpha, (d) Beta and (e) Gamma rhythms, and at the (f) EEGs using DChT.

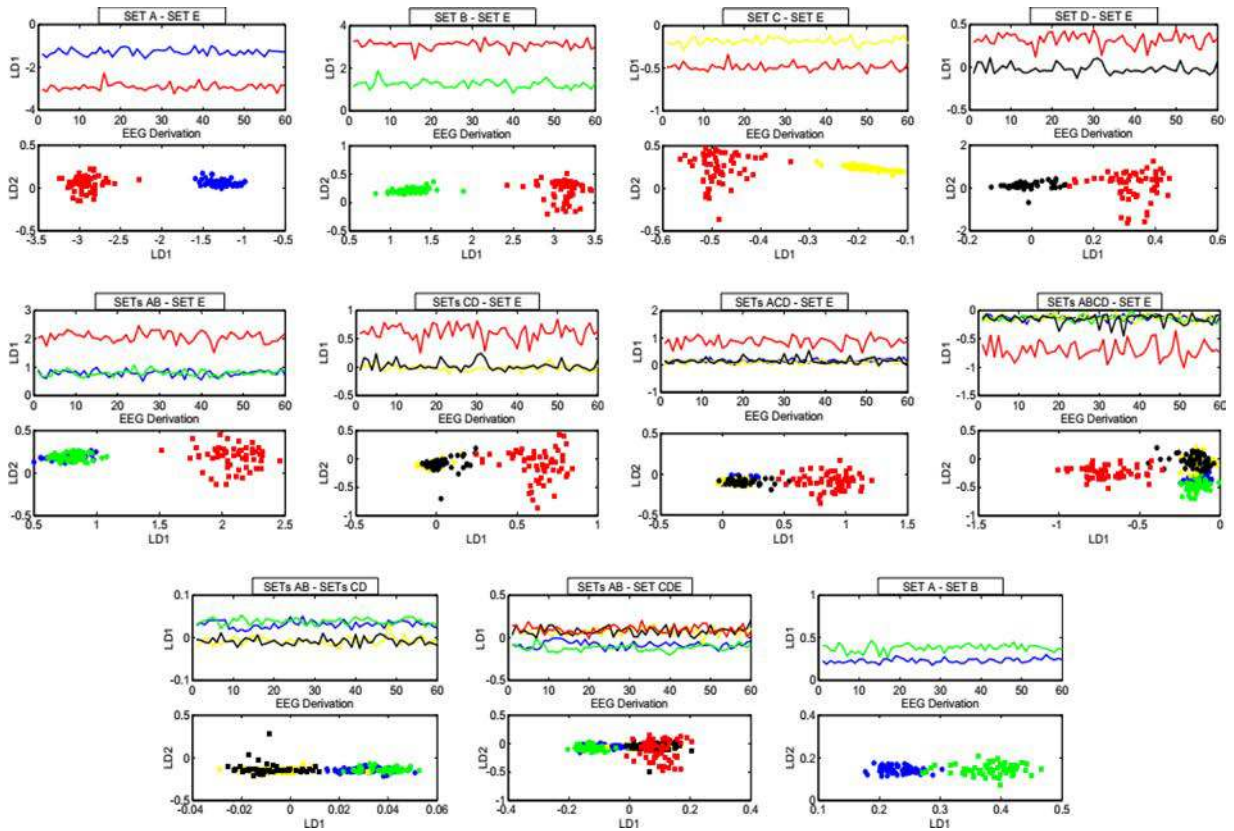


Fig. 8. Comparison of the 1- and 2-dimension DLT features for different experiments after dimensionality reduction using LDA. Colors blue, green, yellow, black and red correspond to SETs A, B, C, D and E, respectively.

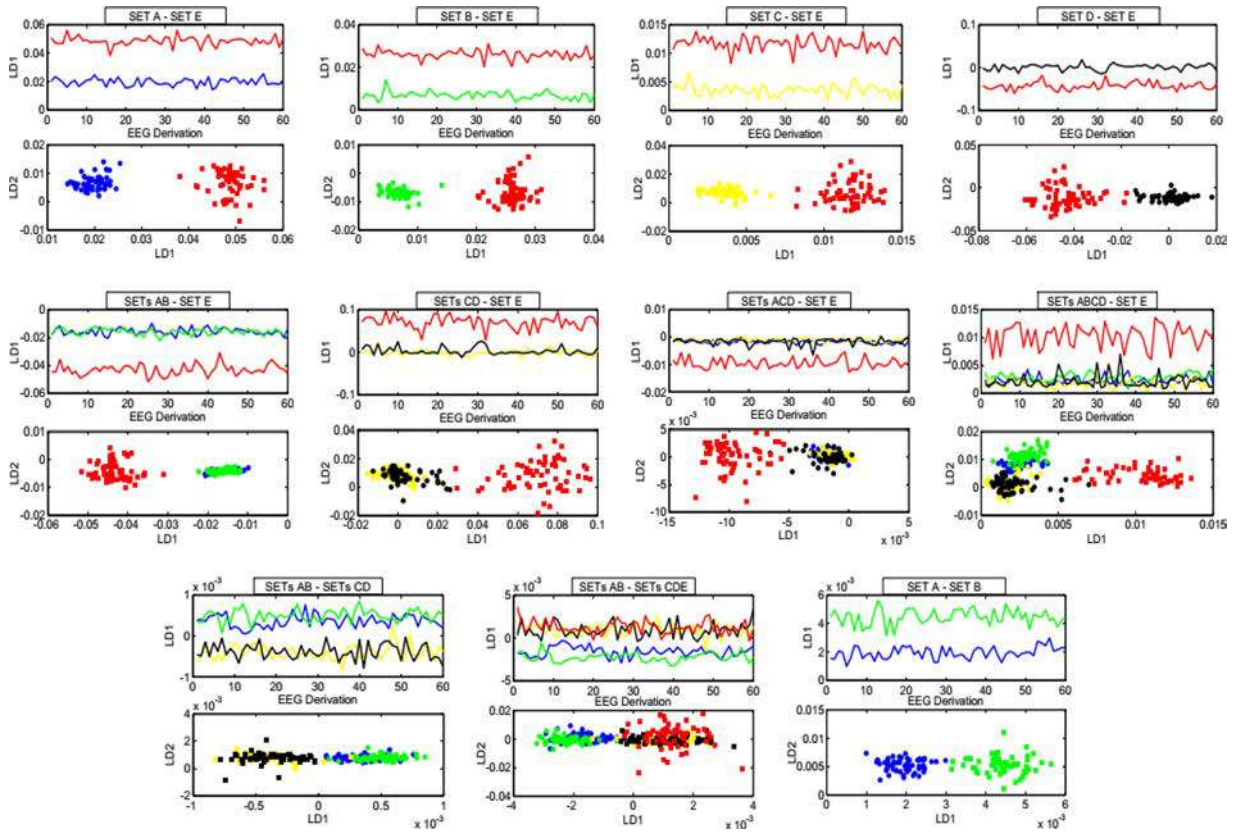


Fig. 9. Comparison of the 1- and 2-dimension DChT features for different experiments after dimensionality reduction using LDA. Colors blue, green, yellow, black and red correspond to SETs A, B, C, D and E, respectively.

**Table 2**  
Seizures detection accuracies for twelve experiments using JPTs-LDA-L-SVM.

Experiment	1-dimension feature		2-dimension feature	
	DLT	DChT	DLT	DChT
A - E	<b>100</b>	<b>100</b>	<b>100</b>	<b>100</b>
B - E	<b>100</b>	<b>100</b>	<b>100</b>	<b>100</b>
C - E	<b>100</b>	<b>100</b>	<b>100</b>	<b>100</b>
D - E	97.50	96.25	<b>98.75</b>	97.50
AB - E	<b>100</b>	<b>100</b>	<b>100</b>	<b>100</b>
CD - E	<b>98.33</b>	<b>98.33</b>	<b>98.33</b>	<b>98.33</b>
ACD - E	<b>99.38</b>	<b>99.38</b>	<b>99.38</b>	<b>99.38</b>
ABCD - E	99.00	<b>99.50</b>	99.00	98.50
AB - CD	96.88	<b>99.38</b>	98.75	98.75
AB - CDE	96.00	<b>97.50</b>	94.50	97.00
A - B	95.00	91.25	<b>96.25</b>	92.50
AB - CD - E (ABCD - E / AB - CD)	98.06	<b>99.44</b>	98.89	98.61
AB - CD - E (AB - CDE / CD - E)	96.88	<b>97.81</b>	95.94	97.50

Bold indicates the highest accuracy for each experiment.

of seizures detection based on permutation entropy (PermEn) and SVM that investigates all the A-E, B-E, C-E and D-E experiments with higher accuracy of 93.55 %, 82.88 %, 88.00 % and 79.94 %, respectively. Also using the dual-tree complex WT and SVM, Anindya et al. [48] gained a 100 % seizures detection accuracy for the A-E, B-E, and C-E experiments, respectively. In order to investigate only the A-E and D-E experiments, Sandeep et al. [49] used the improved PSO and RBF network and achieve higher seizures detection accuracy of 98.00 % and 97.00 %, respectively. Subasi et al. [50] also presented a DWT-PSO-SVM framework that achieves a 99.38 % accuracy in discriminating healthy (A) versus epileptic EEG signals (E). However, Mohd Zuhair et al. [51] used DWT-based ApEn, ANN and LS-SVM to examine all this four experiments, and gained similar results of 100 % seizures detection accuracy like our processing chain. Thus, for this four experiments, it is clearly

**Table 3**  
Seizures detection accuracies for twelve experiments using JPTs-LDA-LS-SVM.

Experiment	1-dimension feature		2-dimension feature	
	DLT	DChT	DLT	DChT
A - E	<b>100</b>	<b>100</b>	<b>100</b>	<b>100</b>
B - E	<b>100</b>	<b>100</b>	<b>100</b>	<b>100</b>
C - E	<b>100</b>	<b>100</b>	<b>100</b>	<b>100</b>
D - E	<b>100</b>	96.25	98.75	97.50
AB - E	<b>100</b>	<b>100</b>	<b>100</b>	<b>100</b>
CD - E	<b>100</b>	98.33	99.17	99.17
ACD - E	<b>100</b>	98.13	98.75	98.13
ABCD - E	<b>100</b>	98.00	99.50	98.50
AB - CD	96.88	<b>99.38</b>	96.88	98.13
AB - CDE	96.00	<b>97.50</b>	96.00	96.00
A - B	<b>96.25</b>	91.25	<b>96.25</b>	91.25
AB - CD - E (ABCD - E / AB - CD)	<b>98.61</b>	<b>98.61</b>	98.33	98.33
AB - CD - E (AB - CDE / CD - E)	97.50	<b>97.81</b>	97.19	97.19

Bold indicates the highest accuracy for each experiment.

demonstrates that our processing chain is accurate than others previously proposed ones.

For the AB-E and CD-E problems, our processing chain extends to be more accurate knowing that Reza Yaghoobi et al. [52] derived a hyperbolic tangent-tangent plot that aims to discriminate SETs C-D EEG signals from SET E with higher accuracy of 92.42 %. This result is less than our obtained 100 % seizures detection accuracy.

For the ACD-E and ABCD-E experiments, we also obtained a highest accuracy of 100 %. This is better than the accuracies obtained by Tzallas et al., Ocak, Ling Guo et al. and Rivero et al. Tzallas et al. [46] examined the ABCD-E experiment with an accuracy of 97.73 %. Ocak [12] also obtains a less seizures detection accuracy of 96.65 % using the discrete WT (DWT) and extracted approximated entropy (ApEn) as input of the ANN for the investigation of the ACD-E experiment. By applying the

**Table 4**

Summary of the highest seizures detection performances using JPTs-LDA-SVM.

Experiment	Seizures detection model	SPE	SEN	ACC
A - E	JPTs - 1- or 2-dimension LDA - L-SVM or LS-SVM	100	100	100
B - E	JPTs - 1- or 2-dimension LDA - L-SVM or LS-SVM	100	100	100
C - E	JPTs - 1- or 2-dimension LDA - L-SVM or LS-SVM	100	100	100
D - E	DLT - 1-dimension LDA - LS-SVM	100	100	100
AB - E	JPTs - 1- or 2-dimension LDA - L-SVM or LS-SVM	100	100	100
CD - E	DLT - 1-dimension LDA - LS-SVM	100	100	100
ACD - E	DLT - 1-dimension LDA - LS-SVM	100	100	100
ABCD - E	DLT - 1-dimension LDA - LS-SVM	100	100	100
AB - CD	DChT - 1-dimension LDA - L-SVM or LS-SVM	100	98.75	99.38
AB - CDE	DChT - 1-dimension LDA - L-SVM or LS-SVM	98.75	96.67	97.50
A - B	DLT - 2-dimension LDA - LS-SVM	95.00	97.50	96.25
AB - CD - E (ABCD - E / AB - CD)	DChT - 1-dimension LDA - L-SVM	100	98.33	99.44
AB - CD - E (AB - CDE / CD - E)	DChT - 1-dimension LDA - L-SVM or LS-SVM	98.13	98.00	97.81

DWT, Ling Guo et al. [13] computed a line length features and used the MLPNN classifier to obtain higher accuracy of 97.75 % and 97.77 % for the ACD-E and ABCD-E experiments, respectively. Rivero et al. [53] also applied the time-frequency analysis and exploited the KNN to only examine the ABCD-E experiment and gained a less seizures detection accuracy of 98.40 %. And with the dual-tree complex WT-based complex valued as inputs of a NN, Peker et al. [54] obtained a 99.15 % accuracy for the ABCD-E seizures detection experiment. However, a closely 100 % accuracy is obtained in [15], where Lina Wang et al. achieved a 99.25 % accuracy for the non-seizure (ABCD) versus seizure (E) experiment using the DWT-based multi-domain feature extraction and SVM classifier. Anindya et al. [48] also investigate the ACD-E experiment and gained a similar 100 % seizures detection accuracy. And Mohd Zuhair et al. [51] with their proposed processing chain also examined the ACD-E and ABCD-E experiments and gained a 100 % and 99.50 % accuracy, respectively.

For the two binary experiments AB-CD and AB-CDE, our processing chain also achieved highest accuracies of 99.38 % and 97.50 % in discriminating healthy (AB) versus seizure-free (CD) and healthy (AB) versus seizure-free + seizure (CDE), respectively. Table 5 also clearly demonstrated that our processing chain is more accurate than the one developed by Reza Yaghoodi et al. [52] which examined the AB-CD problem with a less accuracy of 97.41 %. We also examine the A-B experiment with an acceptable accuracy that can permit to detect whether a patient is with eyes closed or eyes opened. Then, for the AB-CD-E multiclass experiment, Handayani et al. [55] developed a SCICA-PS-ANN model which gained a less accuracy of 94.00 % than the 99.44 % gained by our proposed processing chain.

Overall, it is found that our proposed JPTs-LDA-SVM seizures detection scheme is used to be more efficient and accurate for the A-E, B-E, C-E, D-E, AB-E, CD-E, ACD-E, ABCD-E, AB-CD, AB-CDE, A-B and AB-CD-E experiments with higher seizures detection accuracies of 100 %, 100 %, 100 %, 100 %, 100 %, 100 %, 100 %, 100 %, 99.38 %, 97.50 %, 96.25 % and 99.44 %, respectively. Achieved results demonstrate that the proposed scheme better captured the non-stationarity and non-linearity of EEG signals since the high accuracy is attributed to the highly discriminative features. Then, our proposed JPTs-LDA-SVM

**Table 5**

Comparison of the performance for different experiments with the same data.

Authors	Processing chain	Experiments	ACC (%)
Tzallas et al., 2007 [46]	Time-frequency analysis - ANN	A - E	<b>100</b>
		ABCD - E	<b>97.73</b>
Ocak, 2009 [12]	DWT-based ApEn - ANN	A - E	99.60
		ACD - E	96.65
		A - E	99.60
Ling Guo et al., 2010 [13]	DWT - Line length features - MLPNN	ACD - E	97.75
		ABCD - E	97.77
Rivero et al., 2011 [53]	Time-frequency analysis - KNN	ABCD - E	98.40
Nicolaou et al., 2012 [47]	PermEn - SVM	A - E	93.55
		B - E	82.88
		C - E	88.00
		D - E	79.94
Reza Yaghoodi et al., 2014 [52]	Hyperbolic Tangent-Tangent plot	CD - E	92.42
Handayani et al., 2015 [55]	SCICA - PS - ANN (MLP)	AB - CD	97.41
Peker et al., 2016 [54]	Dual-tree complex WT - Complex-valued - NN	AB - CD - E	94.00
Anindya et al., 2016 [48]	Dual-tree complex WT - SVM	ABCD - E	99.15
		A - E	<b>100</b>
		B - E	<b>100</b>
		C - E	<b>100</b>
		ACD - E	<b>100</b>
Sandeep et al., 2017 [49]	Improved PSO - RBF Network (Gaussian)	A - E	99.00
		D - E	97.00
Lina Wang et al., 2017 [15]	DWT - Multi-domain features extraction - Nonlinear analysis	ABCD - E	99.25
Subasi et al., 2017 [50]	DWT - PSO - SVM	A - E	99.38
		A - E	<b>100</b>
		B - E	<b>100</b>
		C - E	<b>100</b>
		D - E	<b>100</b>
		ACD - E	<b>100</b>
		ABCD - E	<b>99.50</b>
Mohd Zuhair et al., 2017 [51]	DWT - ApEn - ANN/LS-SVM	A - E	<b>100</b>
		A - E	<b>100</b>
		B - E	<b>100</b>
		C - E	<b>100</b>
		D - E	<b>100</b>
		AB - E	<b>100</b>
		CD - E	<b>100</b>
		ACD - E	<b>100</b>
		ABCD - E	<b>100</b>
		AB - CD	<b>99.38</b>
		AB - CDE	<b>97.50</b>
		A - B	<b>96.25</b>
		AB - CD - E	<b>99.44</b>
Sutrisno et al., 2018 [16]	DWT - SD/BP/SE - KNN/SVM/ANN	A - E	<b>100</b>
		A - E	<b>100</b>
		B - E	<b>100</b>
		C - E	<b>100</b>
		D - E	<b>100</b>
		AB - E	<b>100</b>
		CD - E	<b>100</b>
		ACD - E	<b>100</b>
		ABCD - E	<b>100</b>
This paper	JPTs - LDA - SVM	AB - CD	<b>99.38</b>
		AB - CDE	<b>97.50</b>
		A - B	<b>96.25</b>
		AB - CD - E	<b>99.44</b>

Bold indicates the highest accuracy for each experiment.

seizures detection scheme exhibits potential desirable and promising applications for medical treatment as implantable devices to intervene at right time to treat epilepsy. However, it is judicious to note that our processing chain can take more computational time than others processing chains based on fast transforms like WT at the EEG rhythms decomposition stage. This is due to the fact that Jacobi polynomials been continue, the construction of discrete Jacobi polynomials for the modelling of EEG signals is a time consuming process.

#### 4. Conclusion and perspectives

Diagnosing epilepsy is a difficult task requiring the analysis of large amounts of data by an expert, which is tedious, time consuming and can be prone to errors due to fatigue when analyzing by visual inspection. That is why many researchers have focused on the development of computational models for the automatic analysis and detection of epileptic seizures. In this paper, we have proposed a novel processing chain that applied polynomial approach for EEG rhythms decomposition

before feature extraction, dimensionality reduction and classification. Discrete JPTs (DLT and DChT) have been derived using Gauss-Lobatto method and applied to realize efficient EEG rhythms decomposition. Furthermore, LDA is applied on extracted statistical, energy and entropy features for dimensionality reduction, and more informative and discriminative low dimension features are computed and feed as inputs of the L-SVM and LS-SVM with Gaussian RBF kernel for the classification task. Twelve experiments closely related to clinical applications in epilepsy seizures detection are examined and promising results are achieved related to maximum accuracies between 96.25–100 %. Overall, it is found that the proposed processing chain is useful to clinicians for automatic seizures detection and prediction in epilepsy. In addition, the result of EEG signal classification using SVMs shows that JPTs-based

feature extraction combined to dimensionally reduction could improve the performance of classifiers. As prospects, it is necessary to construct fast algorithms of JPTs. Furthermore, randomness as a measure of complexity can be evaluated in order to classify different neurological disorders such as epilepsy, autism and Parkinson diseases. And it would be also interesting to analyze the learning efficiency of these models on the localization of the epileptogenic area.

#### Declaration of Competing Interest

The authors declare that there is no conflict of interests regarding the publication of this paper.

#### Appendix A

Legendre polynomials are Jacobi polynomials for  $\alpha = \beta = 0$ . They are orthogonal on  $[-1, 1]$  with respect to the weight function  $\omega(x) = 1$ . Their three terms recurrence relation and orthogonality relation are defined by Eqs. (A.1) and (A.2), respectively.

$$\begin{cases} L_{i+1}(x) = \frac{2i+1}{i+1}xL_i(x) - \frac{i}{i+1}L_{i-1}(x) , & i = 1, 2, 3, \dots \\ L_0(x) = 1 , & L_1(x) = x \end{cases} \quad (\text{A.1})$$

$$\begin{cases} (L_i, L_j)_\omega = \int_{-1}^1 L_i(x)L_j(x)dx = d_i^2\delta_{ij} \\ d_i^2 = \frac{2}{2i+1} \end{cases} \quad (\text{A.2})$$

Chebyshev polynomials of the 1<sup>st</sup> kind are Jacobi polynomials for  $\alpha = \beta = -1/2$ . They are orthogonal on  $[-1, 1]$  with respect to the weight function  $\omega(x) = (1-x^2)^{-1/2}$ . Their three terms recurrence relation, trigonometric form and orthogonality relation are defined by Eqs. (A.3), (A.4) and (A.5), respectively.

$$\begin{cases} T_{i+1}(x) = 2xT_i(x) - T_{i-1}(x) , & i = 1, 2, 3, \dots \\ T_0(x) = 1 , & T_1(x) = x \end{cases} \quad (\text{A.3})$$

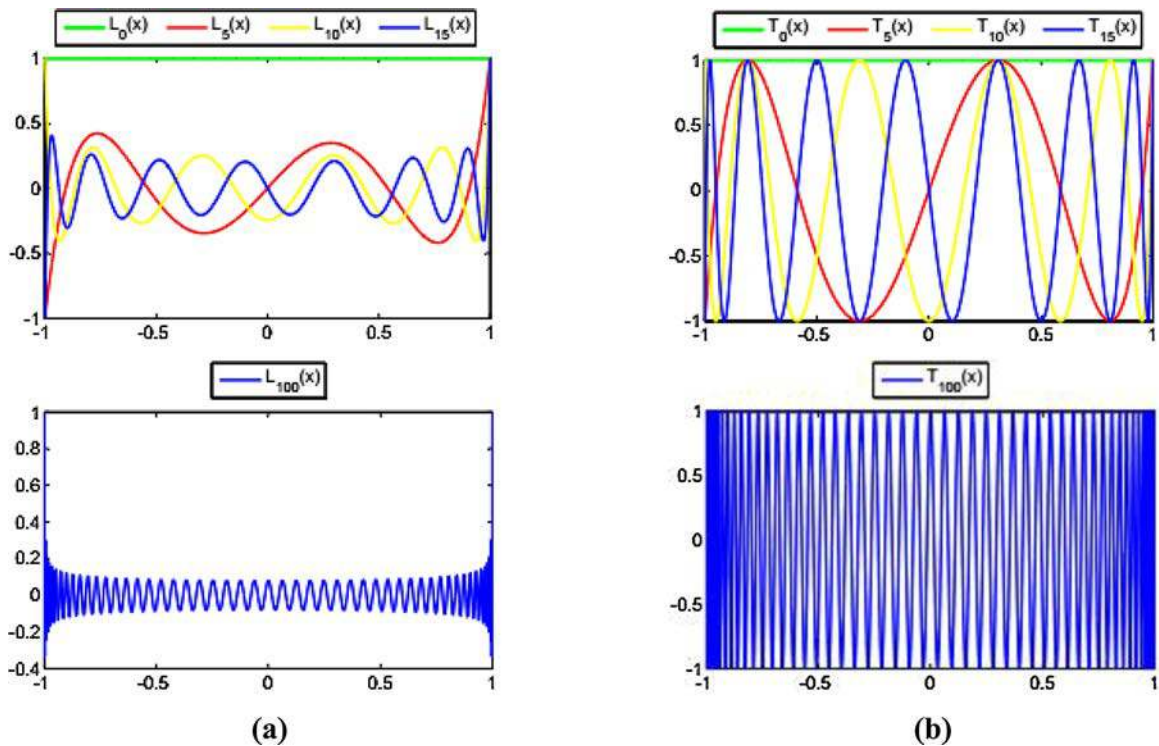


Fig. A1. Curves of some (a) Legendre and (b) Chebyshev polynomials.

$$T_i(x) = \cos[\text{icos}^{-1}(x)] \quad , \quad i \geq 0 \quad (\text{A.4})$$

$$\begin{cases} (T_i, T_j)_\omega = \int_{-1}^1 \frac{T_i(x)T_j(x)}{\sqrt{1-x^2}} dx = d_i^2 \delta_{ij} \\ d_0^2 = \pi \\ d_i^2 = \frac{\pi}{2} \quad , \quad i \geq 1 \end{cases} \quad (\text{A.5})$$

Chebyshev polynomials also satisfy a particular discrete orthogonality relation. If  $x_k$  ( $k = 1, 2, \dots, m$ ) are the exactly  $m$  zeros of  $T_m(x)$  in  $[-1, 1]$ , and if  $i, j < m$ , then:

$$\sum_{k=1}^m T_i(x_k)T_j(x_k) = \begin{cases} 0 & , \quad i \neq j \\ \frac{m}{2} & , \quad i = j \neq 0 \\ m & , \quad i = j = 0 \end{cases} \quad (\text{A.6})$$

With

$$x_k = \cos\left(\pi \frac{2k-1}{2m}\right) \quad , \quad k = 1, 2, 3, \dots, m \quad (\text{A.7})$$

Within the interval  $[-1, 1]$ , Fig. A1 presents the oscillations and changes that occur for Legendre and Chebyshev polynomials having the same frequency as the data set used. It is related that Legendre and Chebyshev polynomials don't change much over time and present similar characteristics to those of stationary signals. Thus, they can be called stationary signals and the FT will be adequate for their analysis [41].

## References

- [1] W. Blume, H. Lüders, E. Mizrahi, C. Tassinari, W. van Emde Boas, J. Engel, Glossary of descriptive terminology for ictal semiology: report of the international league against epilepsy (ILAE) task force on classification and terminology, *Epilepsia* 42 (9) (2001) 1212–1218.
- [2] H. Adeli, Z. Zhou, N. Dadmehr, Analysis of EEG records in an epileptic patient using wavelet transform, *J. Neurosci. Methods* 123 (1) (2003) 69–87.
- [3] Rosenblatt Mariel, et al., A quantitative analysis of an EEG epileptic record based on multiresolution wavelet coefficients, *Entropy* 16 (2014) 5976–6005.
- [4] Muhammad Tariq Salam, Mohamad Sawan, Dang Khoa Nguyen, A novel low-power-implantable epileptic seizure-onset detector, *IEEE Trans. Biomed. Circuits Syst.* (BioCAS) 5 (December 6) (2011) 568–578, <https://doi.org/10.1109/TBCAS.2011.2157153>.
- [5] Karim Abdelhalim, Vadim Smolyakov, Roman Genov, Phase-synchronization early epileptic seizure detector VLSI architecture, *IEEE Trans. Biomed. Circuits Syst.* (BioCAS) 5 (October 5) (2011) 430–438, <https://doi.org/10.1109/TBCAS.2011.2170686>.
- [6] Marjan Mirzaei, Muhammad Tariq Salam, Dang K. Nguyen, Mohamad Sawan, A fully-asynchronous low-power implantable seizure detector for self-triggering treatment, *IEEE Trans. Biomed. Circuits Syst.* (BioCAS) 7 (October 5) (2013) 563–572, <https://doi.org/10.1109/TBCAS.2013.2283502>.
- [7] Wei-Ming Chen, et al., A fully integrated 8-channel closed-loop neural-prosthetic CMOS SoC for real-time epileptic seizure control, *IEEE J. Solid State Circuits* (JSSC) 49 (January 1) (2014) 232–247, <https://doi.org/10.1109/JSSC.2013.2284346>.
- [8] Muhammad Awais Bin Altaf, Chen Zhang, Jerald Yoo, A 16-Channel patient-specific seizure onset and termination detection SoC with impedance-adaptive transcranial electrical stimulator, *IEEE J. Solid State Circuits* (JSSC) 50 (November 11) (2015) 2728–2740, <https://doi.org/10.1109/JSSC.2015.2482498>.
- [9] Muhammad Awais Bin Altaf, Jerald Yoo, A 1.83  $\mu\text{J}$ /Classification, 8-Channel, patient-specific epileptic seizure classification SoC using a non-linear support vector machine, *IEEE Trans. Biomed. Circuits and Syst.* (BioCAS) 10 (February 1) (2016) 49–60, <https://doi.org/10.1109/TBCAS.2014.2386891>.
- [10] Muhammad Rizwan Khan, Wala Saadeh, Muhammad Awais Bin Altaf, A low complexity patient-specific threshold based accelerator for the grand-mal seizure disorder, *IEEE Trans. Biomed. Circuits Syst.* (BioCAS) (October) (2017) 348–351.
- [11] Subasi Abdulhamit, EEG signal classification using wavelet features extraction and a mixture of expert model, *Elsevier Trans. Expert Syst. Appl.* 32 (5) (2007) 1084–1093.
- [12] H. Ocak, Automatic detection of epileptic seizures in EEG using discrete wavelet transform and approximate entropy, *Expert Syst. Appl.* 36 (2) (2009) 2027–2036.
- [13] Ling Guo, Daniel Rivero, Julián Dorado, Juan R. Rabunal, Alejandro Pazos, Automatic epileptic seizure detection in EEGs based on line length features and artificial neural networks, *J. Neurosci. Methods* 191 (2010) 101–109, <https://doi.org/10.1016/j.jneumeth.2010.05.020>.
- [14] Saching Garg, Rakesh Narvey, Denoising and features extraction of EEG signal using wavelet transform, *Int. J. Eng. Sci. Technol.* (IJEST) 5 (June 6) (2013) 1249–1253. ISSN: 0975-5462.
- [15] Lina Wang, Weining Xue, Yang Li, Meilin Luo, Jie Huang, Weigang Cui, Chao Huang, Automatic epileptic seizure detection in EEG signals using multi-domain features extraction and nonlinear analysis, *Entropy* 19 (222) (2017), <https://doi.org/10.3390/e19060222>.
- [16] Sutrisno Ibrahim, Ridha Djemal, Abdullah Alsuwaillem, Electroencephalography (EEG) signal processing for epilepsy and autism spectrum disorder diagnosis, *Biocybern. Biomed. Eng.* 38 (2018) 16–26.
- [17] Atemangho Bruno Peachap, Daniel Tchiotop, Epileptic seizures detection based on some new laguerre polynomial wavelets, artificial neural networks and support vector machines, *Inform. Med. Unlocked* 16 (2019) 1–10, <https://doi.org/10.1016/j.imu.2019.100209>.
- [18] Atangana Romain, Tchiotop Daniel, Kenne Godpromesse, Djoufack Nkengfack Laurent Chanel, Suitable mother wavelet selection for EEG signals analysis: frequency bands decomposition and discriminative feature selection, *Signal Image Process.* – Int. J. (SIPLJ) 11 (February 1) (2020) 33–49, <https://doi.org/10.5121/sipij.2020.11104>.
- [19] Atangana Romain, Tchiotop Daniel, Kenne Godpromesse, Djoufack Nkengfack Laurent Chanel, EEG signal classification using LDA and MLP classifier, *Health Informatics – Int. J. (HIJ)* 9 (February 1) (2020) 14–32, <https://doi.org/10.5121/hij.2020.9102>.
- [20] Abhijit Bhattacharyya, Ram Bilas Pachori, Abhay Upadhyay, U. Rajendra Acharya, Tunable-q wavelet transform based multiscale entropy measure for automated classification of epileptic EEG signals, *Appl. Sci.* 7 (385) (2017), <https://doi.org/10.3390/app7040385>.
- [21] R.B. Pachori, V. Bajaj, Discrimination between ictal and seizure-free EEG signals using empirical mode decomposition, *Res. Lett. Signal Process.* (2008), <https://doi.org/10.1155/2008/293056>.
- [22] Ji Zhong, Qin Shuren, Peng Chenglin, Study on separation for the frequency bands of EEG signal and frequency band relative intensity analysis based upon EMD, in: *Proceedings of the 7th WSEAS International Conference on Signal Processing, Robotics and Automation (ISPRA 08)*, University of Cambridge, UK, February 20–22, 2008. ISSN: 1790-5117 151.
- [23] R.B. Pachori, V. Bajaj, Analysis of normal and epileptic seizure EEG signals using empirical mode decomposition, *Comput. Methods Progr. Biomed.* 104 (2011) 373–381.
- [24] Kai Fu, J. Qu, Y. Chai, Y. Dong, Classification of seizure based on the time-frequency image of EEG signals using HHT and SVM, *Biomed. Signal Process. Control* 13 (2014) 15–22.
- [25] J. Ramakrishnan, Bommanna Raja Kanagaraj, Analysis of non-seizure and seizure activity using intracranial EEG signals and empirical mode decomposition based approximate entropy, *Biomed. Res.* (2017). Vol. Special Issue ISSN: 0970-938X.
- [26] Pushpendra Singh, S.D. Joshi, -R.K. Patney, Kaushik Saha, Fourier-based features extraction for classification of EEG signals using EEG rhythms, *Circuits Syst. Signal Process* 35 (2016) 3700–3715, <https://doi.org/10.1007/s00034-015-0225-z>.
- [27] N. Sivasankari, K. Thanushkodi, Automated epileptic seizure detection in EEG signals using FastICA and neural network, *Int. J. Advance. Soft. Comput. Appl.* 1 (November 2) (2009). ISSN: 2074-8523.
- [28] R.J. Oweis, E.W. Abdulhay, Seizure classification in EEG signals utilizing hilbert-huang, *Transform Biomed. Eng* 10 (38) (2011).
- [29] Ali Yener Mutlu, Detection of epileptic dysfunctions in EEG signals using hilbert vibration decomposition, *Biomed. Signal Process. Control* 40 (2018) 33–40.
- [30] G. Higgins, B. Mc Ginley, S. Faul, R. Mc Evoy, M. Glavin, W. Marnane, E. Jones, The effects of lossy compression on diagnostically relevant seizure information in EEG signals, *IEEE Trans. Biomed. Health Informatics* (BHI) 17 (January 1) (2013) 121–127.

- [31] Pradip Sircar, Ram Bilas Pachori, Rupendra Kumar, **Analysis of rhythms of EEG signals using orthogonal polynomial approximation**, Conference Paper (2009), <https://doi.org/10.1145/1644993.1645025>. January.
- [32] D. Tchiotop, S. Ionita, ECG data communication using chebyshev polynomial compression methods. *Telecomunicatii Numere Publicate, Asociația Generală a Inginerilor din România (AGIR), AN XVI, No 2, 2010*, pp. 22–32. December.
- [33] J. Pardey, S. Robert, L. Tarassenko, A review of parametric modelling techniques for EEG analysis, *Med. Eng. Phys.* 18 (January 1) (1996) 2–11.
- [34] D. Tchiotop, D. Wolf, V. Louis-Dorr, R. Husson, ECG data compression using Jacobi polynomials, *Proceedings of the 29th Annual International Conference of the IEEE EMBS, Lyon France (2007) 1863–1867*. August 23–26.
- [35] R.G. Andrzejak, K. Lehnertz, F. Mormann, C. Rieke, P. David, C.E. Elger, Indications of nonlinear deterministic and finite-dimensional structures in time series of brain electrical activity: dependence on recording region and brain state, *Phys. Rev. E* 64 (6) (2001). DOI: 061907.
- [36] A.V. Nikiforov, V.B. Uvarov, S.K. Suslov, *Classical Orthogonal Polynomials of a Discrete Variable*, Springer-Verlag, Berlin, 1991.
- [37] G. Szego, Orthogonal polynomials, in: *American Mathematical Society Colloquium Publications*, 4th ed., Vol. 23, American Mathematical Society, Providence, RI, 1975.
- [38] Jie Shen, Tao Tang, Li-Lian Wang, **Spectral Method: Algorithms, Analysis and Applications**, Springer-Verlag Berlin Heidelberg, 2011, <https://doi.org/10.1007/978-3-540-71041-7>.
- [39] J.L. Cardenas-Barrera, J.V. Lorenzo-Ginori, E. Rodriguez-Valdivia, A wavelet-packets based algorithm for EEG signal compression, *Med. Inform. Internet Med.* 1 (2004) 15–27.
- [40] G. Higgins, S. Faul, R. Mc Evoy, B. Mc Ginley, M. Glavin, W. Marnane, E. Jones, EEG compression using JPEG2000: how Much loss is too Much? 32nd Annual International Conference of the IEEE EMBS (2010) 614–617.
- [41] T. Tzallas Alexandros, Epileptic seizure detection in EEGs using time-frequency analysis, *IEEE Trans. Inf. Technol. Biomed.* 13 (September 5) (2009).
- [42] A. Subasi, M.I. Gursoy, EEG signal classification using PCA, ICA, LDA and support vector machines, *Expert Syst. Appl.* 37 (2010) 8659–8666.
- [43] Vapnik Vladimir, *The Nature of Statistical Learning Theory*, Springer, New-York, 1995. ISBN: 0-387-94559-8.
- [44] J.A. Suykens, J. Vandewalle, Least squares support vector machine classifiers, *Neural Process. Lett.* 9 (1999) 293–300.
- [45] J.A. Suykens, T. Van Gestel, J. De Brabanter, B. De Moor, J. Vandewalle, *Least Squares Support Vector Machines*, Vol. 4, World Scientific, 2002.
- [46] A.T. Tzallas, M.G. Tsipouras, D.I. Fotiadis, **Automatic seizure detection based on time-frequency analysis and artificial neural networks**, *Comput. Int. Neurosci.* (2007) 1–13, <https://doi.org/10.1155/2007/80510>.
- [47] N. Nicolaou, J. Georgiou, Detection of epileptic electroencephalogram based on permutation entropy and support vector machines, *Expert Syst. Appl.* 39 (1) (2012) 202–209.
- [48] Anindya B. Das, M.I.H. Bhuiyan, S.S. Alam, Classification of EEG signals using normal inverse gaussian parameters in the dualtree complex wavelet transform domain for seizure detection, *Signal Image Video Process.* 10 (2) (2016) 259–266.
- [49] Sandeep Kumar Satapathy, Satchidananda Dehuri, Alok Kumar Jagadev, EEG signal classification using PSO trained RBF neural network for epilepsy identification, *Inform. Med. Unlocked* 6 (2017) 1–11.
- [50] Subasi Abdulhamit, Kevric Jasmin, Canbaz M. Abdullah, **Epileptic seizure detection using hybrid machine learning methods**, *Neural Comput and Applic.* (2017), <https://doi.org/10.1007/s00521-017-3003-y>.
- [51] Mohd Zuhair, Sonia Thomas, Classification of patient by analyzing EEG signal using DWT and least square support vector machine, *Adv. Sci. Technol. Eng. Syst. J.* 2 (3) (2017) 1280–1289. ISSN: 2415-2669.
- [52] Reza Yaghoobi Karimoi, Azra Yaghoobi Karimoi, **Classification of EEG signals using hyperbolic tangent-Tangent plot**, *Int. J. Intelligent Syst. Appl. (IJISA)* 6 (8) (2014) 39–45, <https://doi.org/10.5815/ijisa.2014.08.04>.
- [53] D. Rivero, F.B. Enrique, J. Dorado, A. Pazos, A new signal classification technique by means of genetic algorithms and KNN, in: *Proceedings of the 2011 IEEE Congress of Evolutionary Computation (CEC)*, New Orleans, LA, USA, 2011, pp. 581–586, 5–8 June.
- [54] M. Peker, B. Sen, D. Delen, A novel method for automated diagnosis of epilepsy using complex-valued classifiers, *IEEE Trans. J. Biomed. Health Inf.* 20 (2016) 108–118.
- [55] Handayani Tjandrasa, Supeno Djanali, **Classification of EEG Signals Using Single Channel Independent Component Analysis, Power Spectrum and Linear Discriminant Analysis Advances in Machine Learning and Signal Processing, International Conference on Machine Learning and Signal Processing (MALSIP), 12-14 June, 2015**, [https://doi.org/10.1007/978-3-319-32213-1\\_23](https://doi.org/10.1007/978-3-319-32213-1_23).